Solid State Communications 386 (2024) 115523

Contents lists available at ScienceDirect

Solid State Communications

journal homepage: www.elsevier.com/locate/ssc

Electrical, structural and photovoltaic properties of acceptor dye modified Au/n-Ge heterostructure

D. Mallikarjuna [a], A. Ashok Kumar [a,*], S. Kaleemulla [b,**], V. Rajagopal Reddy [c], M. Raghavender [d], V. Janardhanam [e], Chel-Jong Choi [e]

[a] Department of Physics, YSR Engineering College of YVU, Proddatur, YSR Dist., Andhra Pradesh, India
[b] Thin Films Laboratory, Centre for Functional Materials, Vellore Institute of Technology, Vellore, Tamil Nadu, India
[c] Department of Physics, Sri Venkateswara University, Tirupati, Andhra Pradesh, India
[d] Department of Physics, Yogi Vemana University, Kadapa, YSR Dist., Andhra Pradesh, India
[e] Semiconductor Physics Research Center (SPRC), School of Semiconductor and Chemical Engineering, Jeonbuk National University, Jeonju, 54896, South Korea

ARTICLE INFO

Communicated by: J. R. Chelikowsky

Keywords:
Schottky contact
n-Ge
Heterojunction
Sulforhodamine G
Electrical properties
Organic dye

ABSTRACT

n-Ge heterostructure is fabricated using organic dye interlayers such as sulforhodamine-G (SRG) using low-cost spin coating technique and explored its electrical and structural features. The I–V measurements of the Au/SRG/n-Ge heterostructure (HJ) show good rectification behavior. It has been noticed that the barrier height (0.73 eV) of the Au/SRG/n-Ge heterojunction was significantly higher than the Au/n-Ge Schottky diode (SD) (0.63 eV). Cheung's function and the Norde method has been utilized to evaluate the various barrier parameters to understand the non-ideal behavior of the contacts at higher bias region. The low value of the series resistance for HJ (53 Ω) is observed than compared to the SD without organic dye (2974 Ω). Barrier parameters evaluated from the Norde method were compared with those from the Cheung method and found that they confirmed the consistency of Schottky barrier parameters obtained from both techniques. The transport properties of the HJ and SD in the forward bias region are evaluated using the log (I) vs. log (V) plot. At larger forward bias voltages, a change in the drift of current conduction is observed from Ohmic current conduction to traps-assisted SCLC conduction. This may be ascribed to the presence of defects or traps at the n-Ge and SRG interface possibly associated with the organic dye. Also, the photovoltaic properties of the SRG/n-Ge heterostructures were evaluated at 100 mW/cm^2 showing significant photoresponse indicates the usage of SRG dyes in photosensitive applications.

1. Introduction

In the field of electronic research, Schottky diode fabrication has mostly concentrated on silicon-based semiconductors due to several characteristics of silicon, including its low leakage current, thermal stability, low cost, and high-quality oxide interface. But, as the scaling of Si-based technology faces critical issues, germanium (Ge) is considered a choice of semiconducting material for future generation high-speed CMOS devices due to its symmetric structure and higher carrier mobility than Si and also to overcome the scaling limits of Si-based technological platforms. Furthermore, it is very much compatible with the Si-based CMOS manufacturing process. Unfortunately, the conventional Ge-based devices with metal-semiconductor (MS) Schottky structures face difficulty with the high density of metal-induced gap states (MIGS) at the MS interface, which is caused by strong Fermi-level pinning (FLP) closer to Ge's valence band edge [1–7].This hurdle sets a limit to the device performance, consistency, and steadiness of the Ge-based electronic devices. Numerous device structures was analysed to surmount this problem by inserting interfacial layers (eg. Al_2O_3, TiO_2, SiO_2, ZnO, MgO, Ge_3N_4,TaN) between metal and n-Ge [8–13]. The interlayer between metal and semiconductor reduces the density of the MIGS and prevents the metal wave function from tunneling directly into the semiconductor, this would also enhance the barrier height which causes to reduce the Fermi-level pinning effect and contact resistance [12,14,15]. Janardhanam et al. [16] used O_2 plasma treatment which enabled suppression of Fermi-level pinning of the Al contact to n-type Ge.

Similarly, the addition of an organic interlayer at the metal/Ge

* Corresponding author.
** Corresponding author.
E-mail addresses: drashok.yvuce@gmail.com (A.A. Kumar), skaleemulla@gmail.com (S. Kaleemulla).

https://doi.org/10.1016/j.ssc.2024.115523
Received 24 November 2023; Received in revised form 29 February 2024; Accepted 15 April 2024
Available online 23 April 2024

interface is an added strategy to modulate the Schottky barrier height. A low-cost carbon paste (CP) thin film was coated on n-Ge and studied the electrical properties of the contacts. The use of CP interlayer at the metal-Ge interface shows a highly stable and efficient contact and the device is found to operate even for 500 hrs continuously without degrading its characteristics [2]. Pavani et al. [3] and Jyothi et al. [17] modified n-Ge Schottky contacts using CoPc and pyronine-B organic layers. They determined barrier height from I–V measurements, which were significantly higher than conventional metal/n-Ge contacts. Yildirim constructed Au/n-Ge contacts modified using rubrene interlayer and explored its impact on barrier characteristics [18]. The organic layer between metal-semiconductor junctions greatly affects the electrical characteristics of the contacts. Organic dyes such as methylene blue ($C_{16}H_{18}N_3ClS$), Orange-G ($C_{16}H_{10}N_2O_7S_2Na_2$), and perylene monoamide ($C_{28}H_{24}N_2O_2$) have recently been recognized as very promising conducting materials for various device applications such as electronic devices, including laser diodes, photodetectors, solar cells, microwave sources, and high-speed metal-insulator-semiconductor technology [12,19,20]. On the other hand, few reports are available on the modification of organic/inorganic heterojunctions using the rhodamine group of compounds. An organic interlayer such as rhodamine-101(Rh-101) is used to modify the interfacial properties of n-Si, p-Si and n-InP Schottky structures. Cakar et al. [21] and Gullu et al. [22] studied the influence of Rh-101 organic substance on the barrier properties of n-Si, p-Si and n-InP Schottky structures. They observed the thin layer of Rh-101 exhibits a strong absorption at 565 nm. Further, the enhancement of barrier properties like higher barrier height for the contacts with Rh-101 interlayers was also evidenced. Batir et al. [23] studied about electronic properties of reduced graphene oxide (rGO)-Rh-101 nanocomposite interlayers on p-Si. The barrier properties are found to be enhanced with increasing doping concentration of rGO. Very recently, few researchers reported the use of rhodamine-B (RhB) interlayer influence on the barrier properties of *p*-GaAs [24], p-Si [25] Schottky structures and also reported the usage of RhB thin layers in polymer solar cells as co-sensitizer [26]. Surprisingly, rhodamine-B dye molecules have structural similarities with sulforhodamine-G (SRG) molecules. However, SRG molecules seem to be more fluorescent than RhB molecules. To the best of our knowledge no publications are available on the utilization of sulforhodamine-G (SRG) organic laser dye as an interlayer in the fabrication of organic-on-inorganic heterojunctions. Further, SRG molecules are recognized as acceptor-type ambipolar fluorescent dyes widely used as laser dye material and also in the fabrication of various organic electronic devices.

In the present report, a Au/n-type Ge Schottky contact is modified with a thin organic interfacial layer (SRG) to fabricate organic-on-inorganic heterostructures. The UV–Vis and FTIR studies of the SRG films on glass substrate reveal its structural confirmation and the morphological studies of the SRG thin films on Ge substrate were addressed using FESEM measurements. The electrical properties of these heterostructure were focused using I–V and C–V measurements. Barrier parameters were evaluated and consistency was checked using other different approaches like Cheung's method and Norde method. Finally, it has been demonstrated that the SRG interlayer at the metal-Ge substrate is helpful in the passivation of the Ge surface and also influences the electrical properties of the conventional Au/n-Ge Schottky contacts. Further, the photovoltaic properties of SRG/n-Ge heterostructures have been investigated at 100 W/cm^{2}and the results reveal with 35.23 % fill factor.

2. Experimental methodology

An n-type Ge semiconductor with a carrier concentration of 5×10^{15} cm^{-3} was utilized to fabricate an Au/SRG/n-Ge heterostructure. Initially, the substrate was cleaned in organic solvents using the ultrasonication method for 5 min and washed in DI water. Immediately the Ge-surface is treated with H_2O: HF (100:1) solution to remove the native oxide. Further, the ohmic metallic contact is made by evaporation of aluminium (Al) metal with 50 nm thickness at a vacuum pressure of 5×10^{-6} Torr on the rough side of the n-Ge. The Sulforhodamine-G (SRG) (purchased from Sigma-Aldrich, CAS No.: 230561 with dye content of 60 %) powder was suspended in an organic solvent with a concentration of 10 mg/ml. After ohmic contact formation, SRG organic film was coated on the polished side of the n-Ge substrate using a spin coating approach at 4000 rpm for 60 s and the thickness of SRG layer was found to be ~60 nm as determined from surface profilometer. Afterwards, Schottky metal (Au) was evaporated onto the SRG layer using a shadow metal mask of 500 μm diameter. For comparative studies, using the same process conditions Au/n-Ge Schottky contacts were fabricated without SRG interlayer. The electronic measurements of the Au/SRG/n-Ge and Au/n-Ge Schottky contacts were measured at room temperature using a Keithley 2400 source meter and a precision LCR meter. The properties of the SRG thin films on glass substrate were studied using UV–Vis absorption spectrum and FTIR spectroscopy. The surface morphology of the SRG thin films on the n-Ge substrate was studied using FESEM measurements. Photovoltaic properties of SRG/n-Ge heterostructure were determined using a solar simulator (PECCELL Inc. Japan, PEC-L01) and source meter (Keithley, 2401, USA).

3. Results and discussion

The surface morphology of SRG thin films on Ge substrate is shown in Fig. 1 (a). The surface reveals a needle-like structure and the EDS measurements (not shown here) of the surface exhibits the presence of C, N, S, and Ge elements at the different atomic percentage (shown in the inset of Fig. 1(a)). This confirms the presence of constituent elements of SRG chemical composition. Fig. 1(b) shows the FTIR spectrum of SRG thin film on the glass substrate. The intention of doing the absorption and FTIR measurement of SRG thin films is to understand their optical property which provides the detailed information about the composition and structure of the SRG organic thin film. Preferably, an easiest way to do FTIR measurements of thin films is to deposit them on glass substrates that are transparent in the mid-infrared region. From the spectra, two significant characteristic peaks are observed at 1646 cm^{-1} and 3350 cm^{-1} are recognized as absorption bands of sulforhodamine-G. The characteristic peak at 1646 cm^{-1} might be due to the presence of the carbonyl group (C═O) and the band at 3350 cm^{-1} may be associated with the amine group (-NH). Further, the UV–Vis measurements (absorption spectra) of SRG thin film on a glass plate are shown in Fig. 1(c). It is depicted from the figure that two absorption peaks are observed at 306 nm and 536 nm which were found to be similar to the earlier rhodamine group of materials [23,27]. The optical band gap of the SRG thin film is determined using Tauc relation as defined below [28].

$$(\alpha h\nu)^n = A\left(h\nu - E_g\right) \quad (1)$$

Where the terms involved in the equation such as α is absorption coefficient usually calculated using $\alpha = 2.303(A/t)$ (A is absorption and t is thickness of the film) and E_g is the optical bandgap. The Tauc plot ($(\alpha h\upsilon)^2$ vs. photon energy) shown in Fig. 1(d) was drawn from the absorption spectra revealing an optical bandgap of 1.99 eV. These results were found comparable with rhodamine-101 thin films reported by Cakar et al. [27]. Fig. 1(e) represents the device structure,chemical composition and structure of sulforhodamine-G dye molecules.

Electronic properties of Au/n-Ge contacts with and without the SRG layer measured at room temperature are shown in Fig. 2 (a). The properties exhibit a better-rectifying nature with a considerable reduction in reverse leakage currents of Au/SRG/n-Ge heterostructures. Further, it is also evident that the rectification ratio of the heterostructures is quite improved than the Au/n-Ge contacts. The statistical barrier parameters can be obtained by analyzing the I–V measurement data using thermionic emission (TE) model. The relation between current and voltage by considering the influence of series resistance (R_S)

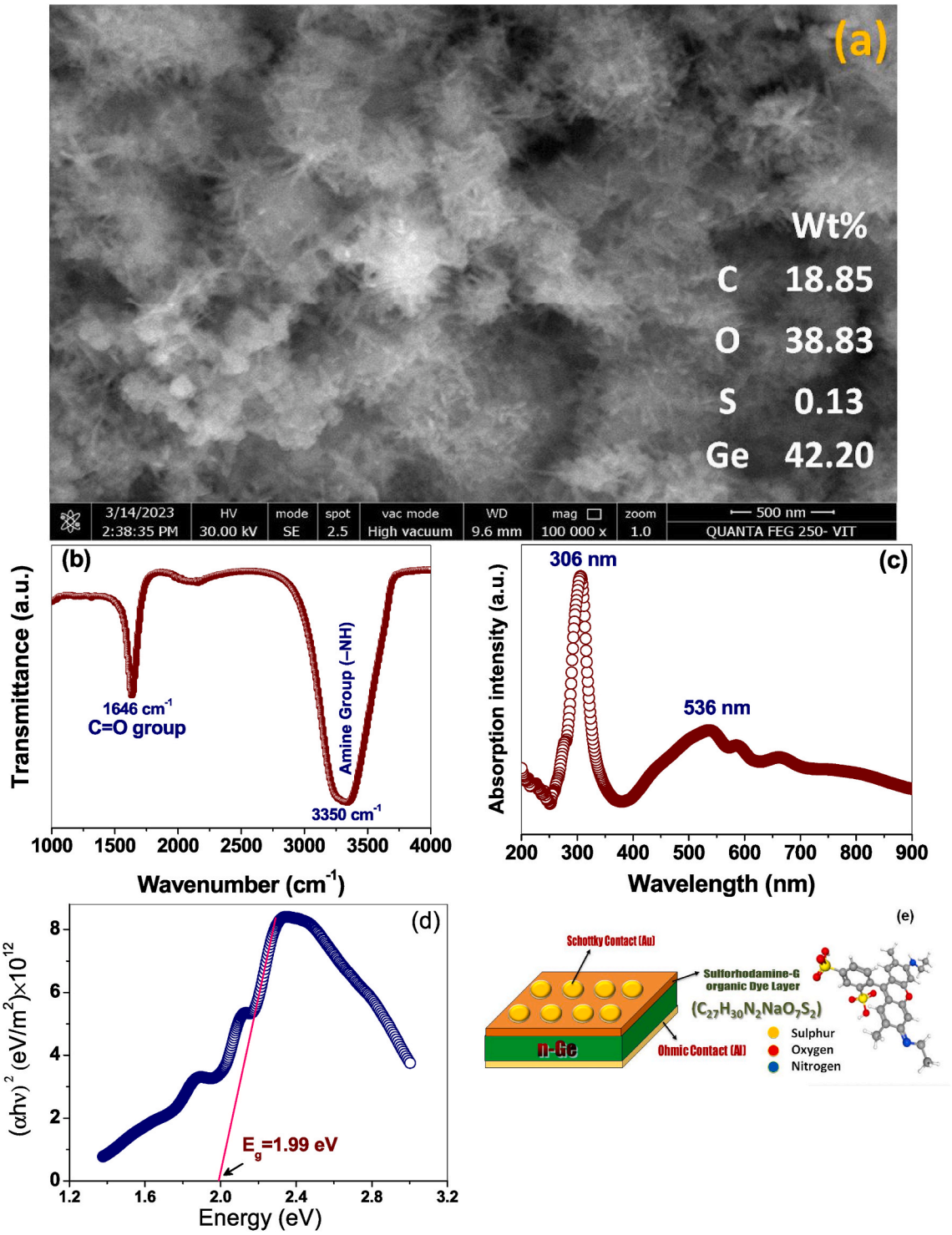

Fig. 1. (a) FESEM image of SRG/n-Ge surface (b) FTIR spectrum of SRG thin film coated on the glass substrate (c) UV-VIS absorption spectrum of SRG thin films coated on the glass substrate (d) Tauc's plot ($(\alpha h\upsilon)^2$ vs. Photon Energy) of SRG thin films (e) Device structure with the chemical formula of SRG and 3-D molecular arrangement.

and interfacial layer can be represented as [29].

$$I = I_o \, exp\left[\frac{q(V - IRs)}{nkT}\right]\left\{1 - exp\left[\frac{q(V - IRs)}{kT}\right]\right\} \quad (2)$$

The terms involved in the above equation have usual meanings [17], the saturation current (I_o) and the ideality factor (n) are obtained from the intercept (at V = 0) and slope of the linear region of ln (current) versus forward bias voltage (V) respectively. The barrier height (Φ_b) can also be evaluated using saturation current and Richardson constant ($A^{**} = 140\ Acm^{-2}K^{-2}$ for n-Ge) [2].The magnitudes of Φ_b and n were found to be 0.63 eV and 1.51 for the Au/n-Ge Schottky contact, and 0.73 eV and 1.30 for the Au/SRG/n-Ge Schottky contact, respectively. The results show that the values of 'n' of both these devices deviated from unity. The magnitudes of ideality factor larger than unity might be ascribed to the existence of SRG layer, arbitrary distribution of dipoles at the interface, and charge transport via traps/interface states [30,31]. On

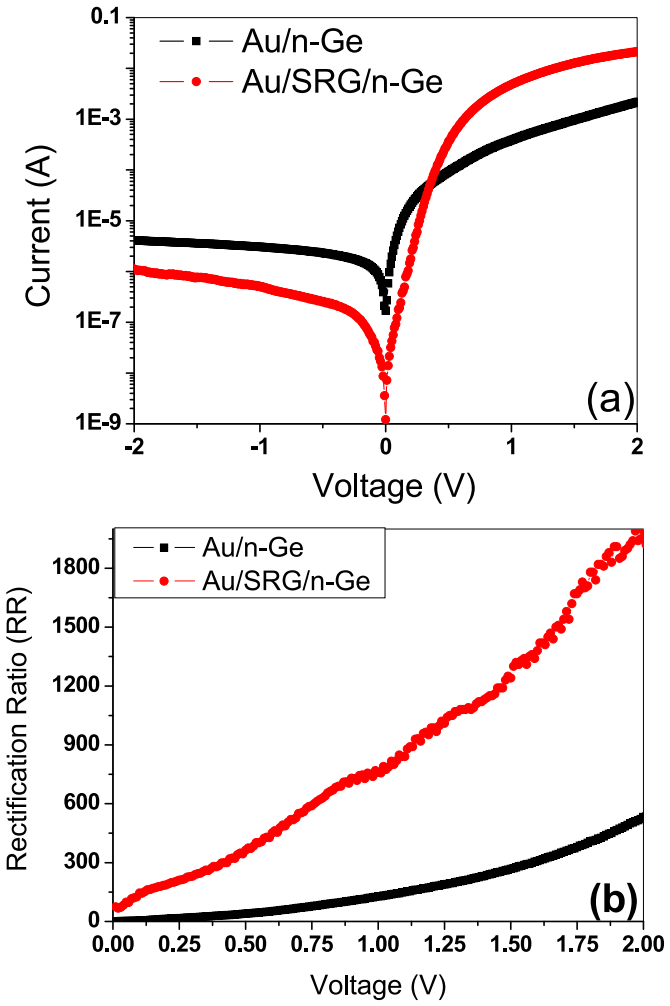

Fig. 2. Electrical properties of Au/n-type Ge and Au/SRG/n-type Ge Schottky contact (a) logarithmic current-voltage properties of contacts (b) Rectification ratio of the contacts with respect to bias potential.

the other hand, the larger ideality factor of the Schottky devices might also be due to secondary mechanisms such as the image-force effect, recombination–generation and tunneling. Further, the larger barrier height observed in SRG/n-Ge contacts specifies the influence of the space charge region of Ge substrate by SRG organic material. However, the SRG organic layer is believed to act as a barrier between Au and Ge substrate, it substantially modifies the Ge surface. The higher barrier height could also be due to organic (SRG) and inorganic (Ge) interface reactivity which possibly changes the band bending at the metal-SRG interface [17]. In general, the variation of organic layer thickness at the metal-semiconductor junction changes the optical bandgap, which further changes the Schottky barrier parameters. The increase in effective area (which is due to thickness variation) helps in the generation and transportation of more charge carriers and thereby leads to high forward currents. Further, an increase in organic layer thickness increases the trapping level energy of the interface states at the organic-semiconductor junction [32,33]. Rectification ratio (RR) of the contacts seems to be essential parameter to quantify magnitude of rectification nature. The RR of the Au/n-Ge and Au/SRG/n-Ge heterostructure shows in Fig. 2 (b) is determined by the ratio of forward current to reverse current for a fixed bias potential. The magnitude of RR for Au/n-Ge contacts is found to be 532 at ±2V and where as for Au/SRG/n-Ge interfaces it is found to be 1990 at ±2V. n-Ge heterojunction with SRG interlayer shows RR increased nearly by 4 times than compared to contact without SRG layer. This shows the superior rectification properties for SRG/Ge heterostructure than compared to Au/Ge contact.

The series resistance (R_S) of the Schottky contacts significantly influences the electronic properties at sufficiently larger forward bias voltages in the non-linear current-voltage data. Cheung's method [34] is a generalized approach to evaluate the R_S of the contact and also the other barrier parameters such as the ideality factor and barrier height for checking the consistency with the ln I versus V approach. Fig. 3 shows Cheung's plots such as dV/d(lnI) versus I and H(I) versus I for the Au/n-type Ge SD and Au/SRG/n-Ge HJ. The dV/d(lnI) versus I plot extracts the R_S from the slope and ideality factor (n) from the y-axis intercept of the plot respectively. The evaluated R_S and n is found to be 3027 Ω and 1.97 for the Au/n-Ge SD and 69 Ω and 2.59 for the Au/SRG/n-Ge HJ. The estimated magnitude of the n has been used in making the H(I) versus I plot which gives a straight line with R_S as a slope and a y-axis intercept yields barrier height (Φ_b). The R_S and Φ_b extracted from the plot of H(I) versus I plot were found to be 2974 Ω and 0.61 eV for the Au/n-Ge SD and 53 Ω and 0.69 eV for the Au/SRG/n-Ge HJ, respectively. The low series resistance observed in the case of SRG/n-Ge interfaces indicates its efficacy in fabricating high-efficiency solar cells and high-speed optoelectronic devices. Smaller R_S and interface state density make the linear behavior of logarithmic (current) vs. voltage plot over a larger bias range (which is evidenced by Fig. 2). A good similarity is observed in the evaluation of R_S from both Cheung's functions.

Norde put forward an empirical model to evaluate the barrier parameters specifically series resistance (R_S) and barrier height of the SD

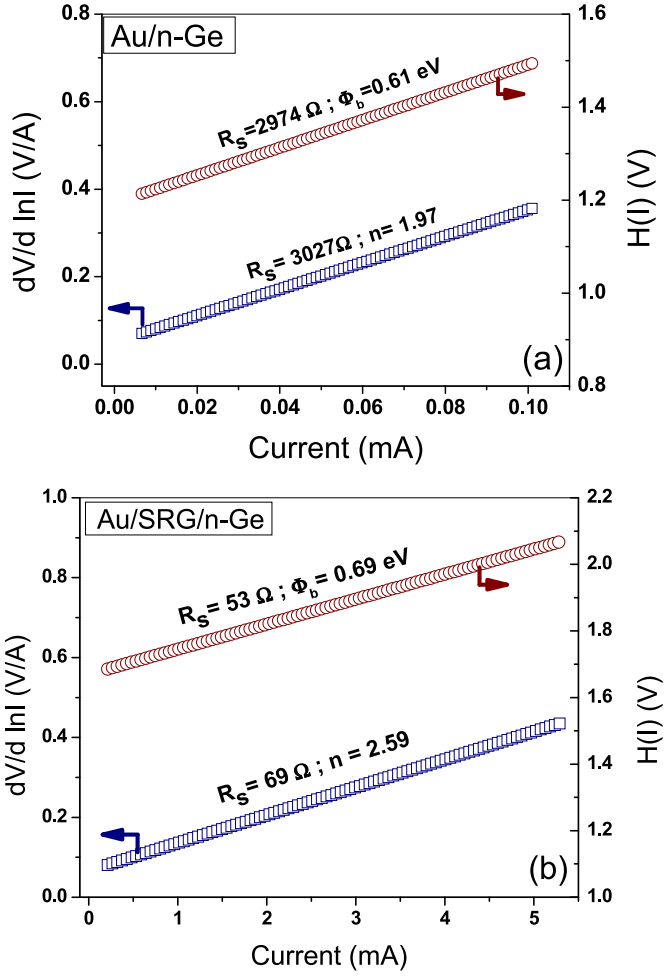

Fig. 3. (a) Plot of dV/d(lnI) versus I and H(I) versus I of Au/n-type Ge and (b) Au/SRG/n-type Ge Schottky contact.

and HJ structures. According to Norde [35], the function F(V) is plotted against voltage (V) to evaluate the barrier parameters. The minimum point in this plot is a matter of interest to identify $F(V_{min})$ and I_{min} which are further used to estimate Φ_b and R_S. Fig. 4 demonstrate the Norde plot of Au/n-Ge SD with and without SRG interlayer. The Φ_b and R_S, extracted from the Norde plot, were found to be 0.63 eV and 2458 Ω for the Au/n-Ge SD, and 0.75 eV and 73 Ω for Au/SRG/n-Ge HJ, respectively. As shown in Table 1, a good uniformity is observed in magnitudes of Φ_b and R_S parameters acquired using different approaches for Au/n-Ge SD with and without SRG interlayer. Evaluation of barrier parameters from various regions of the forward bias I–V plot, however, may account for variations in the Φ_b values for the Schottky structures that were obtained using these various methodologies [36–38]. The variation of Φ_b observed in different approaches such as logarithmic (current) versus voltage, Cheung's and Norde might be due to its evaluation at different regions of the forward bias current-voltage data. Besides, the Φ_b was calculated from the full forward bias I–V characteristics of the Schottky contact in the Norde method.

Fig. 5 shows forward bias I–V characteristics on a double logarithmic scale useful to determine the various current conduction mechanisms of Au/n-Ge SD with and without SRG interlayer. The linear fit of the I–V data on a double logarithmic scale ($I\alpha V^m$) defines the slope factor 'm'. The magnitude of 'm' specifies different possible conduction mechanisms from ohmic to trap-assisted space charge limited current conduction (TCLC). Fig. 5 evidences ohmic conduction, with a slope factor of m = 1.59 (Region 1), is the primary current conduction mechanism observed in the Au/n-Ge SD. Whereas at the higher bias region of the Au/n-Ge SD, the magnitude of slope factor observed as m = 2.61 (Region 2) might also be associated with ohmic conduction due to its square law dependence. On the other hand, in the case of the Au/SRG/n-Ge HJ, three linear regions are observed with different slope factors. It is observed that ohmic conduction is responsible for the linear relationship between current and voltage observed at low bias areas, but the slope increases to rather high values (m = 5.54) in regions of relatively high voltages. At high-bias regions, the current seen in Au/SRG/n-Ge contacts is dominated by a conduction mechanism involving a TCLC. This might be due to the SRG interlayer which induces traps or abnormalities at the contact below the conduction band of the n-Ge semiconductor [17,18]. Finally, the slope factor m = 2.08 was observed at high voltages, which may be attributable to a process of current conduction that is not restricted by traps but rather by space charges.

Capacitance versus voltage measurement is an essential approach for acquiring information about the depletion layer and junction capacitance of Schottky contacts. Fig. 6 depicts the C^{-2} versus V plot of the Au/n-Ge SD with and without SRG interlayer. The Schottky-Mott relationship [2] is used to describe the depletion layer's capacitance.

$$\frac{A^2}{C^2} = \frac{2\left(V_{bi} - \frac{KT}{q} - V\right)}{q\varepsilon_s N_D} \tag{3}$$

where the parameters mentioned above have usual meanings [39]. The doping concentration (N_D), evaluated from the slope of the fitted line of the C^{-2}-V plot, was determined to be 1.64×10^{16} cm^{-3} for Au/n-Ge SD, and 2.19×10^{16} cm^{-3} for Au/SRG/n-Ge HJ, respectively. The measured value of N_D is relatively in good agreement with the carrier concentration of the n-Ge substrate provided by the manufacturer. A doping concentration of a semiconductor is defined based on impurity concentration. Doping is limited by the impurities occupying both acceptor and donor sites, compensating for each other. Redistribution of impurities can also lead to limitations of the maximum doping level in the materials with impurity diffusion strongly depending on the Fermi energy. The Φ_b evaluated from the C^{-2}-V plot was found to be 0.73 eV and 0.81 eV for the Au/n-Ge SD and Au/SRG/n-Ge HJs. The large discrepancy observed in the Φ_b evaluated from the I–V and C–V methods seems to be the sensitivity of these methods to potential fluctuations at the interface [17].

The deviation of exponential behavior at a higher bias range in the forward bias might be associated with the series resistance (R_S) and interface state density (N_{ss}). It is extensively noticed that the magnitudes of N_{ss} shown crucial effect in the electrical behavior of Schottky devices. The distribution of N_{ss} across the interface is plotted against the variation of energy below the conduction band at the forward bias regime by considering voltage-dependent barrier height and ideality factor as follows.

$$N_{ss}(V) = \frac{I}{q}\left[\frac{\varepsilon_i}{\delta}(n(V) - I) - \frac{\varepsilon_s}{W_D}\right] \tag{4}$$

where the parameters mentioned above have usual meanings [17]. The value of W_D is obtained from the experimental C^{-2}-V plots of Au/n-Ge SD and Au/SRG/n-Ge HJ as 1.86×10^{-5} cm and 7.49×10^{-6} cm, respectively. According to Card and Rhoderick [29] and Rhoderick and Williams [40] for n-type semiconductors, surface state energy (E_{SS}) concerning the bottom of the conduction band (E_C) at the semiconductor surface is given by

$$E_c - E_{ss} = q(\Phi_e - V) \tag{5}$$

Fig. 7 shows the N_{SS} has exponentially decreased with the energy of interface states below the conduction band for both Au/n-Ge and Au/SRG/n-Ge HJ diodes. The value of N_{ss} for the Au/n-Ge SD at E_c-0.37 eV is 4.03×10^{14} eV^{-1} cm^{-2} and the Au/SRG/n-Ge HJ at E_c-0.31 eV is 1.69×10^{14} eV^{-1} cm^{-2}. Similarly, the magnitude of N_{ss} for the Au/n-Ge SD at E_c-0.62 eV is found as 3.75×10^{13} eV^{-1} cm^{-2} and, that of Au/SRG/n-Ge HJ at E_c-0.59 eV is found as 8.13×10^{12} eV^{-1} cm^{-2}, respectively. The decreased magnitude of N_{ss} in the case of the SRG/n-Ge interfaces at E_C-0.37 eV than contact without the SRG layer might be associated with the saturation of dangling bonds by the SRG layer.

The photovoltaic property of the SRG/n-Ge HJ is studied using a solar simulator at standard radiation of 100 mW/cm^2 (AM 1 sun solar spectrum). Fig. 8 (a) shows the log (photocurrent) to forward voltage of SRG/n-Ge HJ under dark and illuminated conditions. The photovoltaic property of these contacts under illumination shows a larger photocurrent than compared to dark currents. This signifies the SRG interlayer acts as a photosensitive layer to generate photocurrent at the SRG-Ge junction. The V_{OC} and I_{SC} values of the SRG/n-Ge HJ are obtained as 0.274 μA and 0.053 V respectively. The fill factor of the junction under illumination is recorded as 35.23 %. The produced photovoltaic effect seems to be inferior compared to traditional solar cells. Further, refinement of SRG structure with post-annealing conditions at different

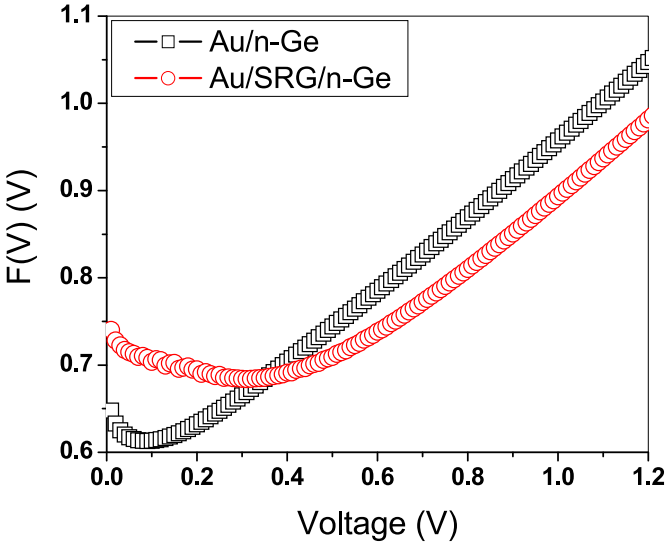

Fig. 4. Norde plot of Au/n-type Ge and Au/SRG/n-type Ge Schottky contact.

Table-1
Schottky barrier parameters extracted by using various methods of Au/n-Ge and Au/SRG/n-Ge HJ Schottky contact.

Devices/Parameters	ln I Vs. V graph		Cheung's Method				Norde Method		C–V Plot
			(dV/dlnI) vs. I		H(I) vs. I				
	n	Φ_b (eV)	$R_s(\Omega)$	n	$R_s(\Omega)$	Φ_b (eV)	R_s (Ω)	Φ_b (eV)	Φ_b (eV)
Au/n-Ge	1.51	0.63	3027	1.97	2974	0.61	2458	0.63	0.73
Au/SRG/n-Ge	1.30	0.73	69	2.59	53	0.69	73	0.75	0.81

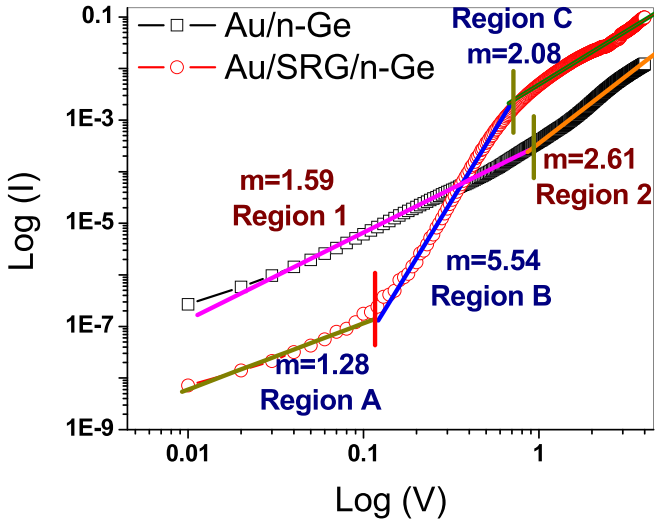

Fig. 5. Forward current conduction mechanisms of Au/n-Ge and Au/SRG/n-Ge contacts.

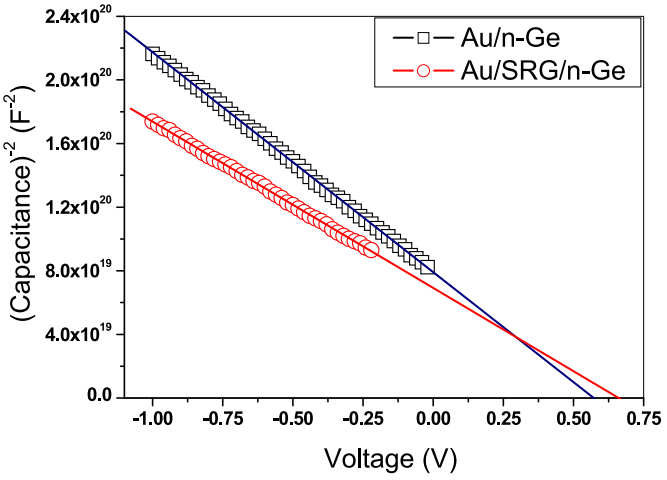

Fig. 6. C–V characteristics of Au/n-Ge Schottky contacts modified with SRG Organic thin layer measured.

atmospheres and doping with various elements may produce a significant change in the photovoltaic parameters [41,42]. Due to their simplicity in fabrication and the possibility of various organic thin layers, metal/organic/inorganic heterostructures show their superiority in the fabrication of photovoltaic cells. Fig. 8 (b) reveals the reliability studies of SRG/Ge heterojunction where the barrier height of the contact was evaluated at different days. These results show a very small variation in the barrier height form its mean value with respect to number of days. This indicates SRG organic substance is utilized in the fabrication of highly stable heterojunction devices. A similar observation is also seen in the fabrication of Pt/carbon paste/Ge heterojunction as reported by Lin et al. [2].

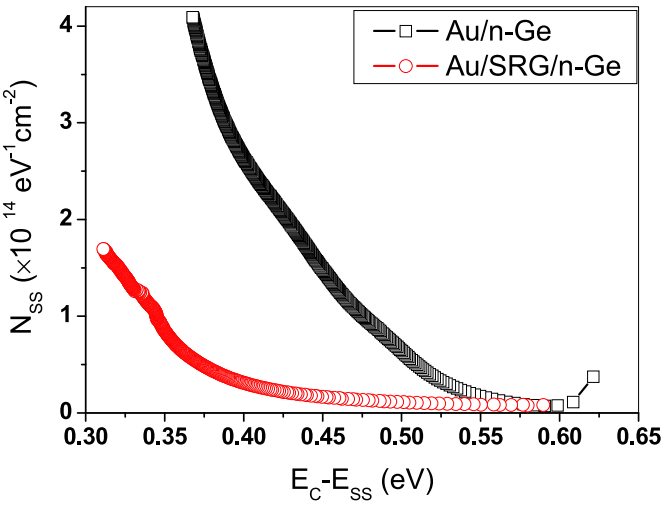

Fig. 7. Energy distribution profiles of N_{SS} for the Au/n-Ge and Au/SRG/n-Ge diodes.

4. Conclusion

In this work, we have investigated the electrical characteristics of the Au/SRG/n-Ge heterostructure (HJ) fabricated by spin coating of the organic dye material on the n-Ge substrate. SRG thin film on the n-Ge substrate showed good rectifying behavior. The evaluated barrier parameters for Au/n-Ge Schottky diode (SD) and Au/SRG/n-Ge HJ reveals that the barrier height value of 0.73 eV obtained for the HJ was found significantly larger than the barrier height value of the conventional SD. The insertion of an organic dye (SRG) thin layer between Au/n-Ge SDs shows a trap-assisted charge-limited current at moderately high bias voltage due to carrier transport via defects or traps at the active layer of the contact below the conduction band. Further, a low series resistance observed in SRG/n-Ge interfaces might show its significant attention in the fabrication of highly efficient solar cells/photovoltaic cells. The distribution of density of surface states is also investigated against the energy of the surface states below the conduction band. The exponential decrease of density of states is observed with the surface state energy in both the contacts. Further, the reduced magnitude of N_{ss} at E_C-0.37 eV in the case of SRG/n-Ge interface than contact without organic layer might be associated with the saturation of dangling bonds at the interface due to organic interlayer. The SRG interlayers show photoresponse at 100 mW/cm^2 with I_{SC},V_{OC} and FF as 0.274 μA, 0.053 V and 35.23 % respectively.

Funding

This research received no external funding.

CRediT authorship contribution statement

D. Mallikarjuna: Writing – review & editing, Writing – original draft, Methodology, Formal analysis, Data curation, Conceptualization. **A. Ashok Kumar:** Writing – review & editing, Writing – original draft,

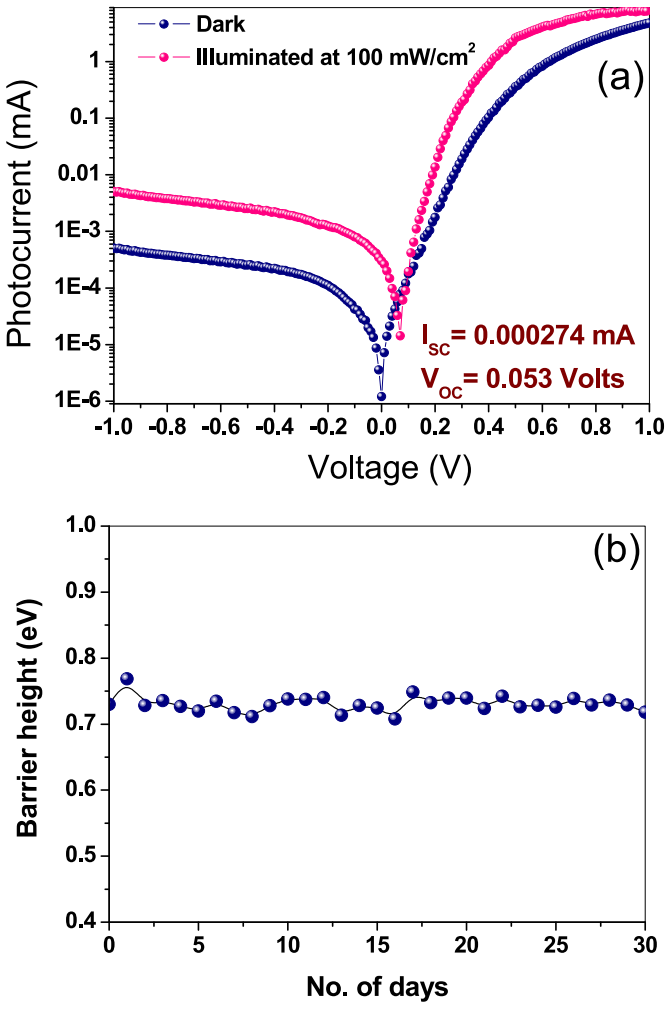

Fig. 8. (a) Photovoltaic Properties of Au/SRG/n-Ge contacts illuminated at 100 Watt/cm^2 optical power under AM 1 sunlight condition (b) Reliability studies of SRG/Ge heterojunction.

Supervision, Methodology, Formal analysis, Data curation, Conceptualization. **S. Kaleemulla:** Writing – review & editing, Methodology, Formal analysis, Data curation. **V. Rajagopal Reddy:** Writing – review & editing, Writing – original draft, Methodology, Formal analysis, Data curation, Conceptualization. **M. Raghavender:** Formal analysis, Data curation. **V. Janardhanam:** Methodology, Formal analysis, Data curation, Conceptualization. **Chel-Jong Choi:** Methodology, Formal analysis, Data curation, Conceptualization.

Declaration of competing interest

The authors declare that they have no known competing financial interests or personal relationships that could have appeared to influence the work reported in this paper.

Data availability

Data will be made available on request.

Acknowledgments

The corresponding authors is grateful to Prof. V. Rajagopal Reddy and Prof. C. J. Choi and their research group for extending fabrication and characterization facilities and also to Dr M. Raghavender, Yogi Vemana University, Kadapa for providing characterization facilities to investigate the photovoltaic properties of Schottky contacts.

References

[1] Z. Wu, W. Huang, C. Li, H. Lai, S. Chen, IEEE Trans. Electron Devices 59 (5) (2012) 1328, https://doi.org/10.1109/TED.2012.2187455.
[2] Pei-Te Lin, Jia-Wei Chang, Syuan-Ruei Chang, Zhong-Kai Li, Wei-Zhi Chen, Jui-Hsuan Huang, Yu-Zhen Ji, Hsueh Wen-Jeng, Chun-Ying Huang, Cryst. Artic 11 (2021) 259, https://doi.org/10.3390/cryst11030259.
[3] M. Tang, H. Cai, Chem. Phys. 530 (2020) 110626, https://doi.org/10.1016/j.chemphys.2019.110626.
[4] S.G. Jung, H.Y. Yu, IEEE J. Electron Devices Soc. 7 (2019) 1119, https://doi.org/10.1109/JEDS.2019.2949566.
[5] J. Wang, W. Huang, J. Xu, J. Li, S. Huang, C. Li, S. Chen, Mater. Sci. Semicond. Process. 91 (2019) 206, https://doi.org/10.1016/j.mssp.2018.11.016.
[6] V. Janardhanam, I. Jyothi, Jong-Hee Lee, Hyung-Joong Yun, Jonghan Won, Yong-Boo Lee, Sung-Nam Lee, Choi Chel-Jong, Thin Solid Films 632 (2017) 23, https://doi.org/10.1016/j.tsf.2017.04.031.
[7] Xuan Luo, T. Nishimura, T. Yajima, A. Toriumi, Japan Soc. Appl. Phys. 113 (2020) 8656, https://doi.org/10.35848/1882-0786/ab7713.
[8] R.R. Lieten, S. Degroote, M. Kuijk, G. Borghs, Appl. Phys. Lett. 92 (2) (2008) 2012, https://doi.org/10.1063/1.2831918.
[9] P.M. Prashanth, Ravi Kesh Mishra, V. Pavan Kishore, Prasenjit Ray, Aneesh Nainani, Yi-Chiau Huang, Mathew C. Abraham, Udayan Ganguly, Saurabh Lodha, Appl. Phys. Lett. 101 (18) (2012) 1, https://doi.org/10.1063/1.4764909.
[10] Y. Zhou, M. Ogawa, X. Han, K.L. Wang, Appl. Phys. Lett. 93 (20) (2008) 2012, https://doi.org/10.1063/1.3028343.
[11] J.Y.J. Lin, A.M. Roy, A. Nainani, Y. Sun, K.C. Saraswat, Appl. Phys. Lett. 98 (9) (2011) 5, https://doi.org/10.1063/1.3562305.
[12] Y.S. Ocak, M. Kulakci, T. Kiliçoğlu, R. Turan, K. Akkiliç, Synth. Met. 159 (15–16) (2009) 1603, https://doi.org/10.1016/j.synthmet.2009.04.024.
[13] K. Martens, R. Rooyackers, A. Firrincieli, B. Vincent, R. Loo, B. De Jaeger, M. Meuris, P. Favia, H. Bender, B. Douhard, W. Vandervorst, E. Simoen, M. Jurczak, D.J. Wouters, J.A. Kittl, Appl. Phys. Lett. 98 (1) (2011) 2012, https://doi.org/10.1063/1.3530437.
[14] Gwang-Sik Kim, Sun-Woo Kim, Seung-Hwan Kim, June Park, Yujin Seo, Byung Jin Cho, Changhwan Shin, Joon Hyung Shim, Hyun-Yong Yu, ACS Appl. Mater. Interfaces 8 (51) (2016) 35419, https://doi.org/10.1021/acsami.6b10947.
[15] J.C. Yang, H.F. Huang, J.H. Li, Y.J. Lee, Y.H. Wang, Vacuum 171 (2020) 108996, https://doi.org/10.1016/j.vacuum.2019.108996.
[16] V. Janardhanam, Hyung-Joong Yun, I. Jyothi, Shim-Hoon Yuk, Sung-Nam Lee, Jonghan Won, Chel-Jong Choi, Appl. Surf. Sci. 463 (2019) 91, 10.1016/j.apsusc.2018.08.187.
[17] I. Jyothi, V. Janardhanam, V. Rajagopal Reddy, C.J. Choi, Superlattice. Microst. 75 (2014) 806, https://doi.org/10.1016/j.spmi.2014.09.016.
[18] M. Yildirim, Politek. Derg 20 (1) (2017) 165, politeknik/issue/36869/420518.
[19] O.F. Yuksel, N. Tuğluoğlu, B. Gulveren, H. Şafak, M. Kuş, J. Alloys Compd. 577 (2013) 30, https://doi.org/10.1016/j.jallcom.2013.04.157.
[20] Ö. Güllü, A. Türüt, Microelectron. Eng. 87 (12) (2010) 2482, https://doi.org/10.1016/j.mee.2010.05.004.
[21] M. Çakar, N. Yildirm, S. Karataş, C. Temirci, A. Türüt, J. Appl. Phys. 100 (7) (2006) 074505, https://doi.org/10.1063/1.2355547.
[22] Ö. Güllü, S. Aydoğan, A. Türüt, Thin Solid Films 520 (6) (2012) 1944, https://doi.org/10.1016/j.tsf.2011.09.043.
[23] G.G. Batir, M. Arik, Z. Caldiran, A. Turut, S. Aydogan, J. Electron. Mater. 47 (1) (2017) 329, https://doi.org/10.1007/s11664-017-5758-4.
[24] M. Soylu, F. Yakuphanoglu, Superlattice. Microst. 52 (3) (2012) 470, https://doi.org/10.1016/j.spmi.2012.05.022.
[25] G.F. Salem, E.A.A. El-Shazly, A.A.M. Farag, I.S. Yahia, Appl. Phys. A 124 (11) (2018) 744, https://doi.org/10.1007/s00339-018-2151-y.
[26] S. Kazemifard, L. Naji, F. Afshar Taromi, J. Colloid Interface Sci. 515 (2018) 139, https://doi.org/10.1016/j.jcis.2018.01.018.
[27] M. Çakar, O. Güllü, N. Yildirim, A. Türüt, J. Electron. Mater. 38 (9) (2009) 1995, https://doi.org/10.1007/s11664-009-0838-8.
[28] A. Tataroğlu, Ş. Altindal, Y. Azizian-Kalandaragh, Phys. B Condens. Matter 576 (2020) 411733, https://doi.org/10.1016/j.physb.2019.411733.
[29] H.C. Card, E.H. Rhoderick, J. Phys. D Appl. Phys. 4 (10) (1971) 1589, https://doi.org/10.1088/0022-3727/4/10/319.
[30] R.T. Tung, Phys. Rev. B 45 (1992) 13509, https://doi.org/10.1103/PhysRevB.45.13509.
[31] I. Jyothi, M.W. Seo, V. Janardhanam, K.H. Shim, Y.-B. Lee, K.-S. Ahn, C.-J. Choi, J. Alloys Comp. 556 (2013) 252, https://doi.org/10.1016/j.jallcom.2012.12.143.
[32] G. Gupta, A. Gundimed, M. Mishra, R. Ahmad, R. Srivastav, U.K. Dwivedi, Indian J. Pure, Appl. Phys. 56 (2018) 468, https://doi.org/10.56042/ijpap.v56i6.15135.
[33] C.Y. Huang, S.Y. Lin, S.S. Cheng, S.T. Chou, C.Y. Yang, T.M. Ou, M.C. Wu, I. M. Chan, Y.J. Chan, J. Vac. Sci. Technol. B 25 (1) (2007) 43, https://doi.org/10.1116/1.2404682.
[34] S.K. Cheung, N.W. Cheung, Appl. Phys. Lett. 49 (1986) 85, https://doi.org/10.1063/1.97359.
[35] H. Norde, J. Appl. Phys. 50 (1979) 5052, https://doi.org/10.1063/1.325607.
[36] Z. Khurelbaatar, Yeon-Ho Kil, Hyung-Joong Yun, Kyu-Hwan Shim, Tae Nam Jung, Keun-Soo Kim, Sang-Kwon Lee, Choi Chel-Jong, J. Alloys Compd. 614 (2014) 323, https://doi.org/10.1016/j.jallcom.2014.06.132.

[37] Y.S. Ocak, R.G. Guven, A. Tombak, T. Kilicoglu, K. Guven, M. Dogru, Philos. Mag. A 93 (17) (2013) 2172, https://doi.org/10.1080/14786435.2013.765985.
[38] A. Ashok Kumar, V. Rajagopal Reddy, V. Janardhanam, Min-Woo Seo, Hyobong Hong, Kyu-Sang Shin, Chel-Jong Choi, J. Electrochem. Soc. 159 (1) (2012) H33, https://doi.org/10.1149/2.041201jes.
[39] S. Mahato, D. Biswas, L.G. Gerling, C. Voz, J. Puigdollers, AIP Adv. 7 (8) (2017) 085313, https://doi.org/10.1063/1.4993553.
[40] E.H. Rhoderick, R.H. Williams, Metal-Semiconductor Contacts, second ed., 1988, p. 124.
[41] N.N. Halder, P. Biswas, S. Kundu, P. Banerji, Sol. Energy Mater. Sol. Cells 132 (2015) 230, https://doi.org/10.1016/j.solmat.2014.08.035.
[42] F.S.B. Kafi, K.M.D.C. Jayathileka, R.P. Wijesundera, W. Siripala, Mater. Res. Express 6 (2019) 085520, https://doi.org/10.1088/2053-1591/ab20b6.